STABILITY AND TRANSPORT PROCESSES IN TOKAMAK PLASMAS

With the macroscopic behavior of tokamak plasmas now reasonably well understood, a major challenge is to develop the physics of plasma turbulence and of the particle and heat fluxes it induces.

James D. Callen, Benjamin A. Carreras and Ronald D. Stambaugh

Tokamak experiments have made dramatic progress over the past two decades, and today plasma parameters are nearing the values needed for a fusion reactor. (See the article by J. Geoffrey Cordey, Robert J. Goldston and Ronald R. Parker on page 22.) In November 1991 the first deuterium–tritium experiments in the Joint European Torus in Abingdon, England, generated a peak fusion power of almost 2 megawatts and a total energy release of 2 megajoules in a 2-second pulse. Concomitant progress has been made in understanding the basic physics of tokamak plasmas; this was made possible by major developments in plasma science, nonlinear theory, plasma diagnostic capabilities and supercomputer calculations.

Twenty years of intensive research on tokamak plasmas have led to a high level of understanding in most of the key areas: charged-particle trajectories, Coulomb collision effects, plasma equilibrium, macroscopic stability and behavior, heating by waves and energetic neutral beams, and the response of the current to momentum inputs. These developments have set the pace for progress in achieving the parameters of tokamak plasmas, and they provide the tools for further improvements to enhance the prospects for a tokamak fusion reactor. The greatest scientific challenge in tokamak physics today is to develop models of plasma turbulence and transport, particularly in the high-pressure, steady-state operational regimes of the future. This article describes the progress that has been made in understanding and controlling macroscopic instabilities (see figure 1) and in investigating microinstabilities and the plasma turbulence and transport fluxes they induce.

James Callen is Donald W. Kerst Professor in the department of nuclear engineering and engineering physics and in the department of physics at the University of Wisconsin, Madison. **Benjamin Carreras** is an ORNL Corporate Fellow in the fusion energy division of Oak Ridge National Laboratory. **Ronald Stambaugh** is director of the boundary physics and technology division of the fusion group at General Atomics in San Diego.

Requirements for fusion

The requirements for net fusion energy production set the plasma physics goals for a tokamak reactor. A magnetically confined deuterium–tritium plasma will yield net fusion energy if it is both:

▷ hot enough that fusion collisions between nuclei are sufficiently probable relative to elastic Coulomb collisions (an ion temperature T_i of 10 keV, or 10^8 K, gives a probability of about 1%, which is sufficient)

▷ well enough confined that the energy loss rate is less than the fusion power (the product of the plasma ion density n and the plasma energy confinement time τ_E must be at least 10^{20} sec/m^3).

In addition, the plasma density must be of order 10^{20} ions/m^3 so that the fusion energy produced per unit volume is large enough for attractive fusion economics but does not present too large a power and neutron flux load on the first wall surrounding the plasma. The implied volume-average plasma pressure $\bar{p}$ is small compared with the energy density of the magnetic field that confines it; their ratio β, defined as $\bar{p}/(B^2/2\mu_0)$, is 0.03 when B is 5 T. The following minimum plasma parameters needed for magnetic fusion energy have now all been achieved: $T_i \geq 10$ keV, $n \geq 10^{20}$/m^3, $\tau_E \geq 1$ sec and $\beta \geq 0.03$. The requirements for an economical fusion reactor are somewhat higher, as the article on page 22 explains.

A plasma of density 10^{20} ions/m^3 and temperature 10 keV is a nearly fully ionized, quasineutral gas of charged nuclei and electrons. The ions and electrons will be in the plasma state in which charged-particle interactions are

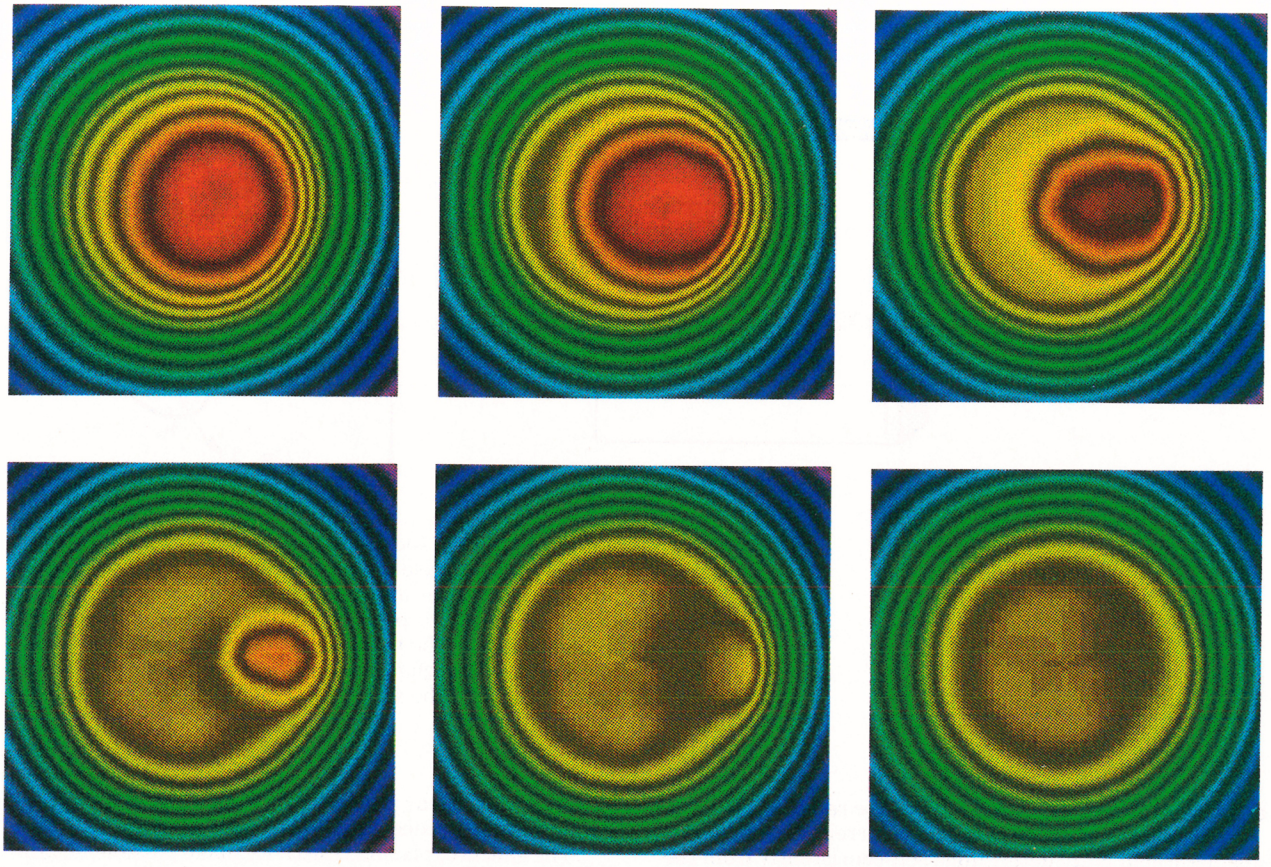

Electron temperature isotherms measured during a "sawtooth crash" in the central region of a plasma in the Tokamak Fusion Test Reactor at the Princeton Plasma Physics Laboratory.[21] Red represents the highest temperature, 6000 eV; the separation between isotherms is 500 eV. The relaxation shown takes about 3 milliseconds; the fourth and sixth frames are separated by only about 130 microseconds. During the "crash" the hot core of the plasma moves from inside to outside the crescent-shaped region, or island, evident in the second through fourth frames. After the heat escapes the central region, it becomes distributed homogeneously just outside the original island. (Courtesy of Yoshio Nagayama, Kevin McGuire and Alfred Cavallo, Princeton Plasma Physics Laboratory.) **Figure 1**

predominantly collective rather than binary.[1] (The number of interacting charged particles is about 10^8, which is approximately the number of particles within the Debye shielding distance of about 0.1 mm.) In tokamaks, magnetic fields are used to confine the fast-moving charged particles, which have speeds of about 10^6 m/sec. Perpendicular to magnetic field lines, the Larmor or gyro orbits of the ions are less than about 4 mm; this is small compared with the plasma radius, which is greater than about 1 m. Parallel to the magnetic field, confinement is provided by having the magnetic field lines close on themselves.

Magnetic field structure in equilibrium

The tokamak concept of magnetic confinement was invented independently in the early 1950s by Igor E. Tamm and Andrei D. Sakharov[2] and by Lyman Spitzer.[3] Magnetic field lines in a tokamak lie on the surfaces of nested toroidal doughnuts,[4] as indicated in figure 2. They are produced by a combination of toroidal (ζ) and poloidal (θ) magnetic field components: $\mathbf{B} = \mathbf{B}_\zeta + \mathbf{B}_\theta$, where ζ and θ are angular variables corresponding respectively to the long and short ways around the torus. The equilibrium magnetic geometry is assumed to be axisymmetric: $\partial B/\partial\zeta = 0$. The magnetic field lines twist helically around the torus on a magnetic flux surface Ψ, defined by $\int \mathbf{B}_\theta \cdot d\mathbf{S} = \text{constant}$. The field lines have a winding number, or plasma stability "safety factor," given by

$$q(\Psi) \equiv \left.\frac{d\zeta}{d\theta}\right|_\Psi \simeq \frac{rB_\zeta}{R_0 B_\theta}$$

Here r and R_0 are the minor and major radii of the flux surface. (The magnetic field structure in a tokamak is equivalent to the phase space orbits of a Hamiltonian system where the angle ζ represents time, the magnetic flux Ψ is energy, and $1/q$ is the frequency of motion around the torus; the nonlinear dynamics theory of Hamiltonian systems is used to explore the effects of perturbations of the axisymmetric equilibrium magnetic field.) Rational magnetic flux surfaces are those on which the winding number q is the ratio of two integers, m/n, and the magnetic field lines close periodically on themselves after circumnavigating the torus poloidally n times for every m toroidal transits. On irrational surfaces, where $q \neq m/n$, magnetic field lines cover the magnetic flux surfaces ergodically. In typical tokamak plasmas $q(\Psi)$ ranges from slightly less than unity near the center of the plasma to about 3–4 at the edge of the plasma. The "pitch" B_θ/B_ζ of the helical magnetic field lines is approximately $r/R_0 q$. Because the small pitch changes from the center to the edge of the plasma, the magnetic field is sheared, causing

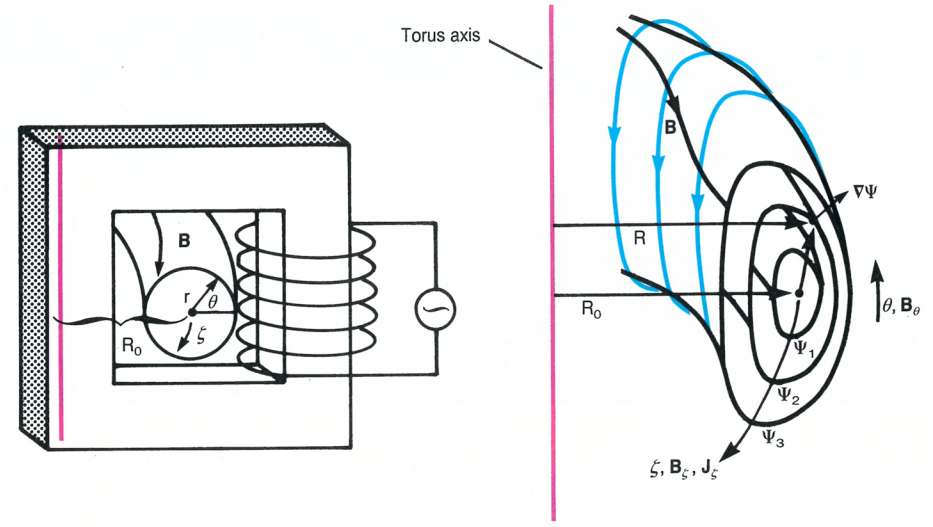

Magnetic geometry in early (left) and modern (right) tokamaks. In the toroidal direction ζ the magnetic field component $\mathbf{B}_\zeta$ in the modern design is produced by currents in coils (blue) around the torus in the poloidal direction θ. The poloidal magnetic field $\mathbf{B}_\theta$ is produced by the current $\mathbf{J}$, which flows mostly toroidally in the plasma. The toroidal current $\mathbf{J}_\zeta$ is induced primarily by a changing magnetic flux through the central hole of the toroidal doughnut. This current provides the secondary "winding" for the ohmic heating transformer. **Figure 2**

any helically resonant instabilities to be radially localized.

The spatial distributions of the current density $\mathbf{J}$ and magnetic field $\mathbf{B}$ are determined self-consistently from the magnetohydrodynamic equilibrium equations: the force balance $\nabla p = \mathbf{J}\times\mathbf{B}$ and the magnetostatic Maxwell equations $\nabla\times\mathbf{B} = \mu_0\mathbf{J}$ and $\nabla\cdot\mathbf{B} = 0$. For an axisymmetric tokamak these equations can be combined to yield a nonlinear elliptic partial differential equation for the magnetic flux Ψ in terms of the pressure distribution and the poloidal current distribution—the Grad–Shafranov equation.[5] The boundary conditions are provided by the transformer-induced poloidal magnetic field outside the plasma. This field must include a vertical component to prevent the current-carrying plasma loop from expanding radially. Current practice is to solve the Grad–Shafranov equation numerically to determine the physical location of the magnetic flux surfaces—the surfaces where $\Psi(r,\theta)$ is constant—in a way that is self-consistent with the experimentally measured pressure profile p and the magnetic field imposed outside the plasma. This equilibrium description is the basis for systems that control the shape of tokamak plasmas in real time. Such systems now routinely produce equilibria with complicated, temporally evolving cross-sectional shapes to better than about 1-cm accuracy.

Instabilities in tokamak plasmas

While the axisymmetric equilibrium is well behaved, we must also consider deformations of the plasma that break the toroidal symmetry and that may be states of lower energy. The most virulent of these instabilities arise in the "ideal" magnetohydrodynamic description of plasmas, in which the effects of plasma resistivity are vanishingly small in the short time scale of interest. Such instabilities lead to gross force-balance mismatches that grow on the very fast time scale of the Alfvén time, which is on the order of microseconds. These rapidly growing modes can limit the operating space of tokamaks by causing a loss of plasma energy throughout the tokamak in less than a millisecond. Linear theory is adequate for determining the conditions needed to stabilize these modes.

The effects of plasma resistivity make possible instabilities that grow more slowly, on a millisecond time scale; these involve diffusive reconnection (or tearing) of the magnetic field lines. These resistive MHD tearing modes evolve nonlinearly into magnetic islands—bifurcations of the magnetic topology—that usually saturate at a size under 10 cm but can still degrade plasma confinement. Most experiments are able to avoid such modes by controlling the plasma current profile.

On a finer spatial scale the plasma allows a spectrum of saturated, low-level, radially localized instabilities. The turbulence from these microscopic modes is thought to produce the observed anomalously high level of cross-field, or "radial," heat transport. To examine these instabilities and their effects requires a full nonlinear, multimode plasma turbulence treatment. The remainder of this article discusses what is known about the three classes of instabilities mentioned above—ideal MHD, resistive MHD and microscopic modes—focusing on their effects and their control or amelioration.

Limits set by ideal MHD stability

Ideal magnetohydrodynamic stability is usually assessed through trial fluid-element perturbations $\tilde{\boldsymbol{\xi}}(\mathbf{x})$, which induce magnetic field distortions $\tilde{\mathbf{B}}_1 \simeq \nabla\times(\tilde{\boldsymbol{\xi}}\times\mathbf{B}_0)$, where $\mathbf{B}_0$ is the equilibrium magnetic field. (The tilde indicates a perturbation.) The perturbations are examined to see how they change the potential energy of the system.[6] A perturbation that lowers the potential energy of the system indicates a growing instability in the plasma. The displacement from equilibrium will occasion a conservative perturbed force $\tilde{\mathbf{F}}(\tilde{\boldsymbol{\xi}})$ and a change in plasma potential energy

$$\delta W = -\frac{1}{2}\int \tilde{\boldsymbol{\xi}}\cdot\tilde{\mathbf{F}}(\tilde{\boldsymbol{\xi}})\,d^3x$$

Excitation of shear or compressional Alfvén waves or

sound waves in a plasma increases the potential energy ($\delta W > 0$) and leads to decaying perturbations. However, perturbations that tap the free energy associated with the pressure gradient or the plasma current can lower the potential energy ($\delta W < 0$) and hence lead to instabilities. Figure 3 shows typical perturbation structures for these two types of instabilities. These results were obtained from numerical solutions of the Euler–Lagrange equations derived from conservation of kinetic plus potential energy. For ideal MHD instabilities the induced magnetic perturbation is "frozen into" the perfectly conducting plasma fluid and deforms the shapes of the magnetic flux surfaces but does not change their topology. The growth rates of these modes are scaled by the poloidal Alfvén time, about 0.1 μsec, and hence are very fast. The fast growth of these modes, coupled with the fact that their effects can extend over the entire plasma (as shown, for example, in figure 3), shows that the ideal MHD instabilities can be quite virulent and generally must be avoided.

Three types of ideal MHD instabilities are possible in tokamaks:

▷ *Vertical instabilities* of the plasma column are stabilized in circular-cross-section plasmas by an externally imposed vertical field that has concave curvature on the outboard side of the toroidal plasma. However, plasmas with highly elliptical cross sections are unstable (though only at the rather slow 10-msec time scale on which the magnetic field diffuses into the vessel wall surrounding the plasma) since vertical fields with small or convex curvature are used to vertically elongate the plasma. A major success of the 1980s was the development of poloidal-field feedback systems capable of controlling vertical instabilities in plasmas with highly elliptical cross sections.

▷ *Kink instabilities* that helically contort the plasma column can occur in tokamak plasmas at low pressures.[6] Fortunately these virulent instabilities, which tap the plasma-current free energy, are limited to small domains in the value of q_{edge}, the winding number at the plasma edge. For a constant-current-density model these domains of q_{edge} lie just below integer values. For the distributed-current profiles more typical of tokamak plasmas, unstable modes occur mainly when $q_{edge} \lesssim 2$ (see figure 3a), and this translates into an upper bound on the maximum current in the plasma.

▷ *Pressure-gradient-driven instabilities* in ideal MHD plasmas are caused by "bad curvature"—concave toward the plasma—of the helical magnetic field lines within the plasma on the outboard side of the torus. (These fluid-element "interchange" instabilities are similar to Rayleigh–Taylor fluid instabilities, with the field-line curvature playing the role of gravity and pressure the role of density.) However, because magnetic field lines "spend more time" on the inboard side where there is good curvature, the average curvature is good for $q \gtrsim 1$. Hence the "interchange" instabilities with $\tilde{\xi}$ constant along magnetic field lines do not grow in normal ($q \gtrsim 1$) tokamak plasmas.[6] However, the $\tilde{\xi}$ perturbation can concentrate, or "balloon," in the outer "bad curvature" region, but in so doing it induces a magnetic perturbation $\tilde{\mathbf{B}}_{1\perp}$. A ballooning instability, which is shown in figure 3b, is possible if the local pressure-gradient drive exceeds the magnetic "bending" energy $\tilde{\mathbf{B}}_{1\perp}{}^2/2\mu_0$. In plasmas near this instability limit with optimized pressure and winding-number profiles, these modes are barely avoided throughout the entire plasma. For these optimum plasmas the "critical" ratio β of the average plasma pressure to the energy density of the magnetic field that confines the plasma is well described by the relation[7]

$$\beta_{crit}(\%) = fI/aB \qquad (1)$$

where the plasma current I is in megamps, the plasma's

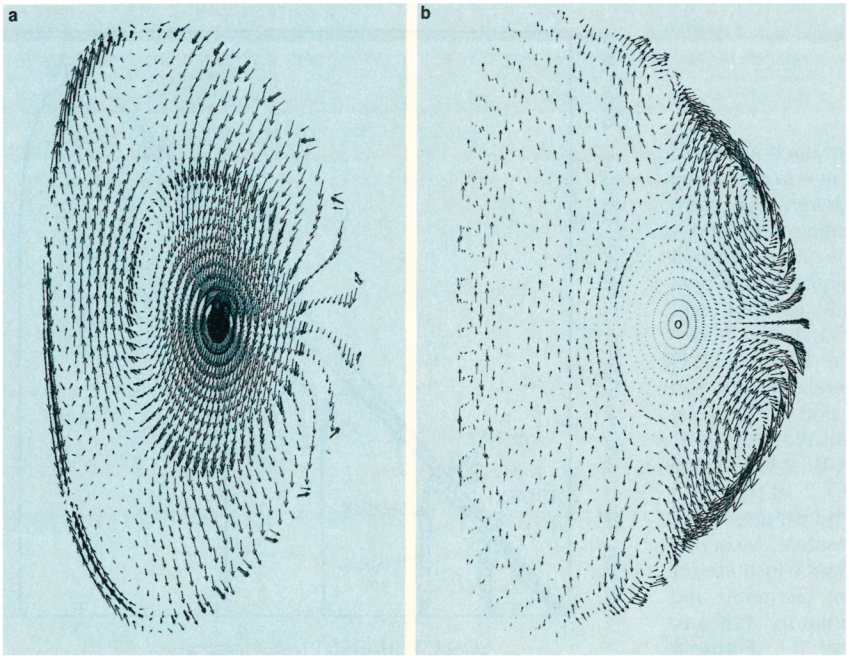

Instability displacement vectors $\tilde{\xi}$ within the plasma cross section plane at one toroidal azimuth. **a:** An $n = 1$ dominantly current-driven instability with $q_{edge} \approx 2$. **b:** A dominantly pressure-driven instability near the β limit. The current-driven mode shows a dominant component for which $m/n = 2/1$. The pressure-gradient-driven mode "balloons" at the outer midplane. These results were obtained with the GATO computer code.[22] **Figure 3**

minor radius a is in meters, and the magnetic field strength B is in teslas. The coefficient f, which is about 2.8–4.4 depending on the nature of the instabilities, is a weak function of the ellipticity, triangularity and other parameters of the plasma cross section.

The scaling in equation 1, together with the kink mode limitation $q_{edge} < 2$ on the plasma current, implies that the limit for the ratio β, or pressure, can be increased mainly by increasing the ratio of current to minor radius and hence by making the plasma cross section highly elongated or triangular. Nearly circular plasmas in the early 1980s showed β limits of about 3%. In the late 1980s, three more highly noncircular tokamaks—DIII-D in San Diego, PBX-M in Princeton and JET in England, all equipped with heating powers of up to 20 MW—have increased the achieved ratio β, as theoretically expected.[8] In figure 4, the stable operating space is shown for the tokamaks that have been used to investigate high ratios β. Equation 1 with a coefficient f of 3.5 gives a good description of the limit for the ratio β, or pressure, for all these devices.[8] Also, the ratio β is limited by a combination of ballooning modes and kink modes, in agreement with the theoretical predictions.

Ballooning stability theory predicts that for high-β or high-pressure equilibria in which the low-shear regions are moved to regions of more favorable curvature, access to a so-called second stability regime of much higher ratios β is possible, particularly with D-shaped or indented "kidney bean" plasma cross sections.[9] Some experiments have flirted near this regime, but the kink modes there remain a problem. The plasma discharge from which figure 3b was derived is one such example. Recent calculations have optimized the profiles by putting the maximum pressure gradient at radii where the shear is large, yielding the prediction that ratios β up to $5.5\,I/aB$ can be stable to kinks. Such high normalized β values have been achieved in the PBX-M and DIII-D tokamaks. Thus, although agreement on the β limit is sufficient to allow the design of future devices, and although the achieved values well exceed fusion reactor requirements, there is still room for further improvement in β.

Deuterium–tritium fusion reactions in a tokamak reactor will generate another free-energy source for instability of ideal MHD modes: a significant number of energetic α particles. These particles are born at such a high energy—3.52 MeV—that there can be a population of them whose velocities parallel to the magnetic field lines exceed the Alfvén speed. This α-particle population introduces a new free-energy source in δW that can destabilize ideal MHD modes via a Čerenkov-type effect. To explore this new physics will require plasmas that burn enough deuterium and tritium to produce a large population of α particles.

Resistive MHD instabilities

The small electrical resistivity in a tokamak makes possible additional collective macroscopic instabilities,[10] albeit with much longer growth times of 10^{-4}–10^{-2} sec. These times are, however, still quite short compared with the energy confinement time τ_E of about 1 sec. The additional modes result from the diffusion or tearing of magnetic field lines relative to the plasma fluid, such that the magnetic field is no longer "frozen in." Thus resistive MHD instabilities do not preserve the nested topology of the magnetic flux surfaces. They produce nonlinear "magnetic islands" within the plasma, as seen in figures 1 and 5.

The Lundquist number, or magnetic Reynolds number, is the ratio of the magnetic diffusion time to the poloidal Alfvén time. Present tokamak plasmas have very large Lundquist numbers of 10^7–10^9. As a result, their high electrical conductivity constrains perturbations to be ideally magnetohydrodynamic—that is, topology preserving—throughout most of the plasma. However, for helically resonant magnetic field perturbations, magnetic field diffusion can dominate the ideal MHD effects in very thin boundary layers around surfaces that have a rational winding number. Reconnection of the magnetic field lines in these layers produces a nonaxisymmetric magnetic island that forms a helical structure within the plasma, as

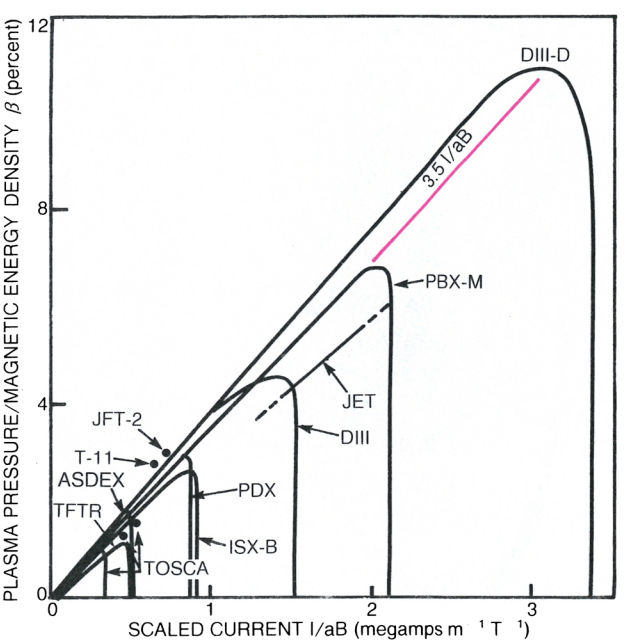

Stable operating space for each indicated tokamak lies below the corresponding curve. A pressure-driven limit, often accompanied by ballooning-type modes with low mode numbers, is encountered at about $\beta = 3.5\,I/aB$ in all these high-beta experiments. The vertical line to the right in each case is approximately the "kink" limit at $q_{edge} = 2$ for that device. DIII-D and DIII are at General Atomics, San Diego; PBX-M, PDX and TFTR, at the Princeton Plasma Physics Laboratory; JET, in Abingdon, England; ISX-B, at Oak Ridge National Laboratory; JFT-2, at the Japan Atomic Energy Research Institute, Naka; T-11, at the Kurchatov Institute, Moscow; ASDEX, at the Max Planck Institute for Plasma Physics, Garching, Germany; and TOSCA, at Culham Laboratory, Culham, England. (Adapted from ref. 8.) **Figure 4**

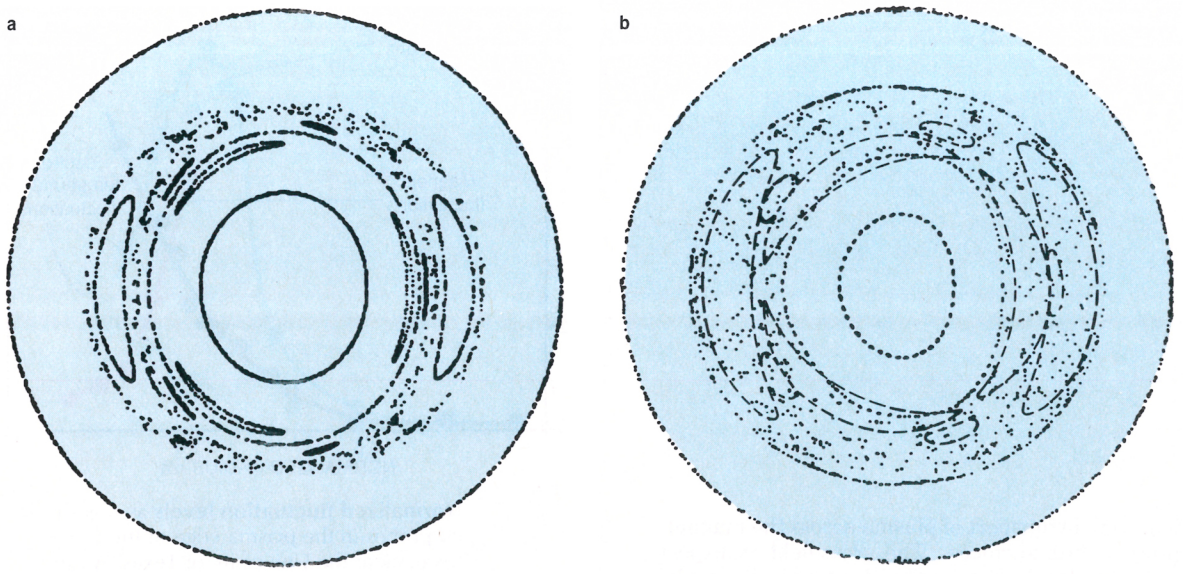

Magnetic field structure just before (**a**) and during (**b**) the initial stage of a major disruption in the plasma current. These "puncture plots" follow a few magnetic field lines many times around the torus; the dots indicate places where the lines puncture the cross section on their toroidal transits. At the early time (**a**), the separated $m/n = 3/2$ and $2/1$ magnetic islands are evident and separated by a KAM surface. At the later time (**b**), these magnetic islands overlap and the magnetic field lines become stochastic over the entire region originally occupied by both islands. (From J. D. Callen *et al.*, ref. 10.) **Figure 5**

seen in figures 1 and 5.

In tokamaks, only modes of low m and n (such as $m/n = 1/1$, $2/1$, $3/1$, $3/2$ and so on) are unstable to resistive MHD instabilities. Ultimately, the helical magnetic island caused by a given unstable mode usually becomes much wider than the resistive boundary layer. The island grows slowly until it acquires all the accessible free energy associated with the current and then saturates—except for the $m/n = 1/1$ mode, which is a more global mode that usually induces a topological inversion where the hottest part of the plasma moves from inside to outside the island, as in figure 1.

For tokamak plasmas operating well within the ideal MHD limits on q and β discussed above, the nonlinear evolution of resistive MHD modes with low m and n provides models for the most important macroscopic phenomena observed in tokamak plasmas: the sawtooth behavior of the central electron temperature (the $m/n = 1/1$ mode), the steady magnetic islands that are sometimes present within the plasma (2/1 or 3/1 modes) and the abnormal major disruptions, or terminations, of the plasma current (the overlap of the 2/1 and 3/2 modes, as shown in figure 5).

Figure 1 shows a 1/1 island structure observed during a "sawtooth crash" relaxation event in the Tokamak Fusion Test Reactor at Princeton. (TFTR is shown on the cover of this issue.) The initial growth of the magnetic island is well described by resistive MHD, but the highly nonlinear crash phase is not understood. Sawtooth crashes can be delayed or prevented by adding a fast-ion plasma component or by modifying the current profile near the $q = 1$ magnetic surface.

The nonlinear evolution of low-order resistive MHD instabilities in tokamaks is typically calculated using computer codes that advance the highly nonlinear resistive MHD equations, which are difficult to solve because the magnetic Reynolds number is so large. Figure 5, the result of such a numerical calculation, shows the magnetic field lines in a tokamak just before and during a major disruption of the plasma current.

The 2/1 and 3/2 magnetic islands are clearly present in part a of the figure, and they are well separated from each other and from the rest of the plasma by magnetic flux boundaries known as KAM (Kolmogorov–Arnold–Moser) surfaces. Stochastic magnetic field lines are clearly evident, but only in small regions near the boundaries of the magnetic islands.

In part b of the figure the islands have clearly overlapped, and the field lines have become stochastic throughout a large region of the plasma. At this point the modes are growing explosively. Comparisons of simulations of this type with experimental results have shown good agreement with a number of features of major disruptions in tokamaks: broadening of the current profile, reduction in plasma inductance and an externally observed negative voltage spike. Fortunately, experimenters are able to reduce the occurrence of major disruptions to a small percentage of discharges. Disruptions of this type and of the ideal MHD kink type can also be controlled (at least theoretically and in some small-scale experiments) through external feedback circuits that impose, on the time scale of the mode's linear growth, helically resonant magnetic fields that counter those generated in the plasma.

Tokamak experiments can now be run for long periods of time without any of the macroscopic instabilities discussed here being present, except possibly the central-region sawteeth. While resistive MHD theory provides models for the basic phenomena, kinetic effects can be important nonlinearly and in plasmas with significant fast-ion components such as those due to alpha particles from deuterium–tritium fusion.

Plasma turbulence and transport

The confinement of plasmas in tokamaks operated stably with regard to macroscopic phenomena is determined by

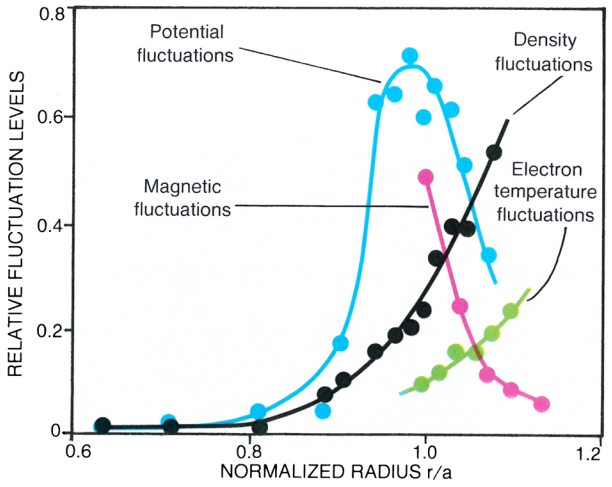

Normalized fluctuation levels as measured by probes in the plasma edge of the TEXT tokamak at the University of Texas, Austin. The relative fluctuation levels of the potential $\tilde{\phi}$, density $\tilde{n}$ and electron temperature $\tilde{T}_e$ are high—up to 70%—in the edge of the plasma ($r \sim a$) but drop below 1% in the hot core of the plasma ($r \lesssim 0.8\,a$). The magnetic fluctuations $\tilde{B}_r$ are much smaller; they are apparently largest in the core of the plasma. The potential fluctuation level drops sharply as the poloidal velocity shear layer at $r \sim 0.95a$ is crossed going inward. (Adapted from ref. 13). **Figure 6**

the residual radial transport of plasma across the magnetic field lines or flux surfaces. The cross-field transport occurs at a low level that is found empirically to be adequate, but not optimal, for a tokamak reactor. However, that level is anomalously high compared with what Coulomb collision effects alone would produce, and it is not well understood.[11]

The hot plasma core is only weakly "collisional," because the mean free path between 90° scatterings due to the cumulative small-angle Coulomb collisions is typically over two orders of magnitude larger than the $2\pi R_0$ toroidal length of a tokamak, which is about 16 m in TFTR. The magnetic field strength varies along the helical magnetic field lines in a tokamak and is highest on the inside of the torus and lowest on the outside. This variation creates magnetic mirrors that trap the low-collisionality charged particles with small parallel velocities on the outer, low-field side of the torus. Only untrapped electrons carry the parallel current in response to the toroidal electric field and other current-driven momentum inputs. The parallel current is impeded by collisional friction with ions and by viscous drag on poloidal flows produced by collisions with the trapped particles. Experimentally the parallel current is found to be governed solely by Coulomb collision effects.

Perpendicular to the magnetic field lines, charged particles both gyrate in their Larmor orbits and drift cyclically off magnetic flux surfaces. Coulomb collisions between particles following these trajectories cause radial diffusion. The effects induced by gyro motion are called classical diffusion, while the larger, drift-orbit-induced effects, due primarily to trapped particles, are called neoclassical diffusion.[12] For electrons, theoretical estimates of both of these perpendicular transport processes are usually at least two orders of magnitude smaller than the experimentally inferred values. Thermal diffusivities of ions, however, can sometimes be as low as the neoclassical prediction. Thus in tokamaks the parallel transport processes seem to be governed by Coulomb collision effects, but the perpendicular transport processes are usually anomalous and are presumably dominated by microturbulence effects in the plasma.

In discussing plasma turbulence and transport, it is important to distinguish between two plasma regions: the core and the edge.[13] (See figure 6.) At the plasma edge, studies on the MACROTOR tokamak at the University of California, Los Angeles, showed that the fluctuations are, in general, very large—on the order of the equilibrium quantities—and dominantly electrostatic, meaning that they have negligible magnetic components. From measurements using externally inserted metallic probes, it has been inferred in an experiment in the TEXT tokamak at the University of Texas, Austin, that particle transport at the edge can be explained as the local fluctuation-induced transport.[13] In contrast to the situation for the edge plasma, fluctuation levels in the core are low and may have a significant magnetic component. Measuring fluctuations and transport processes in the hot core plasma is much more difficult than in the edge. Consequently, the experimental picture of fluctuations and transport in the core is only beginning to be developed, and the information needed to correlate core transport with fluctuations is not yet available.

Edge

In the theoretical analysis of edge-plasma turbulence, it is possible to use fluid-like equations. The processes that generate short radial-scale-length plasma microinstabilities, and hence vorticity, in the edge can be quite complex. The plasma is not fully ionized in this region, and thus there are effects due to radiation cooling, ionization and charge-exchange interactions with neutrals. These effects tend to reinforce extant microinstabilities, generate new ones and create larger relative fluctuation levels in the edge than in the hot plasma core.[14]

Changes in edge turbulence and transport can significantly affect the overall confinement of plasmas in tokamaks by their effects on the boundary conditions for the core plasma. Recently the large radial electric field at the plasma edge and its effect on confinement have attracted a great deal of attention and effort in tokamak research.[15–18] A radial electric field induces a predominantly poloidal $\mathbf{E}\times\mathbf{B}/B^2$ flow that advects turbulent

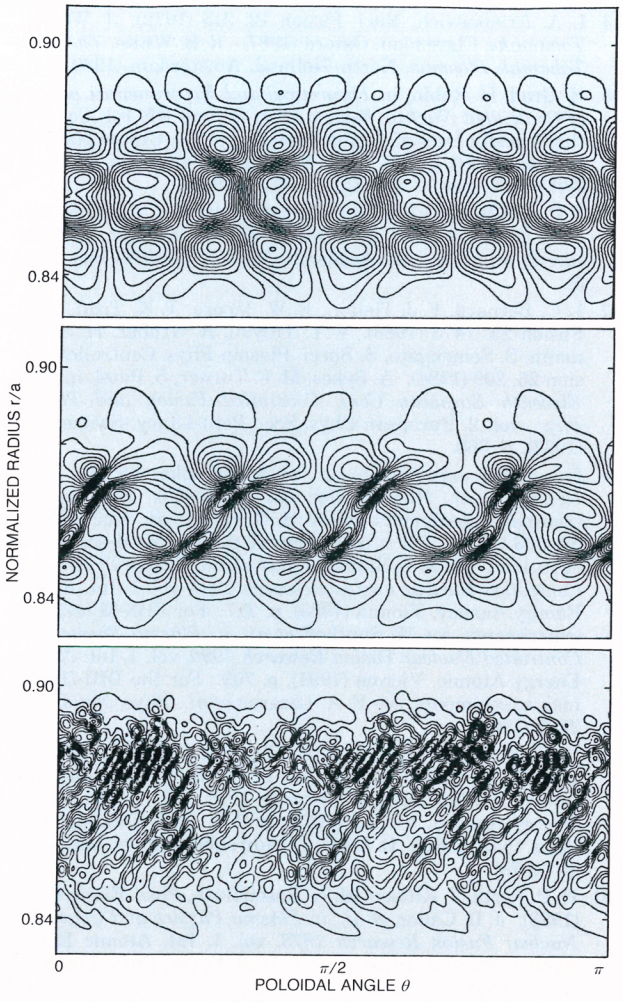

Edge plasma turbulence, from numerical calculations. The three frames show the plasma's self-consistent evolution from an initial state dominated by coherent modes (top) through a strongly sheared flow state (middle) to a final state where the turbulent eddies are broken up by the sheared flow (bottom). (From ref. 23.) **Figure 7**

vortices in the poloidal direction θ. (Advection is transport by flow.) The next derivative, a radial gradient in the electric field, causes shear in this poloidal flow, which tends to shear apart turbulent vortices.

The relation between poloidal flows and turbulence is complex, involving flow generation due to turbulent Reynolds stresses and shear flow amplification due to radial propagation of the turbulence, a dynamo-like effect.[15] Nonetheless, when the poloidal flow shear is sufficiently large it can reduce both the decorrelation time and radial scale size (see figure 7) of the turbulent eddies in the plasma. This diminishes the turbulence level and the induced radial plasma transport. While there is still some controversy about the nature of the underlying plasma turbulence and precisely how the poloidal flow affects it, these sheared-poloidal-flow effects on edge turbulence and transport are thought to be generic and have been observed experimentally.

Thus a change in the poloidal flow shear in the plasma edge has been proposed as the trigger for the transition from "low mode" confinement to an enhanced "high mode" confinement regime that has a transport barrier at the edge.[16] Experimental evidence from DIII-D shows a close correspondence among increased flow shear, turbulence suppression and transport reduction.[17] Also, experiments in the CCT tokamak at the University of California, Los Angeles, have shown that when enough current is drawn out of the edge of a tokamak plasma that the induced $\mathbf{J}\times\mathbf{B}$ poloidal force exceeds the collisional poloidal flow damping,[12] a large radial electric field and a large poloidal flow are induced, and the plasma changes from low- to high-mode operation.[18] More fundamentally, recent experimental studies in TEXT have shown that the decorrelation time of the edge turbulence is reduced in the edge velocity-shear layer.[14] In addition, the density profile steepens at the same radius, which indicates that the local diffusion coefficient is also reduced and that the sheared poloidal flow produces an edge transport barrier. Hence strong poloidal flow shear in the edge can significantly control turbulent plasma transport there and enhance overall tokamak plasma confinement.

Core

Plasma turbulence and transport in the hot plasma core are more difficult to analyze because many more kinetic and nonlinear effects can operate there. The free-energy sources that drive plasma microinstabilities, and hence microturbulence, are primarily the radial pressure and temperature gradients in both the electron and ion species. The gradients are a natural consequence of confinement. Models of tokamak plasma microturbulence range from small-scale, drift-wave-like instabilities, which extend over a few gyro radii ρ_i of ions ($\rho_i \lesssim 4$ mm), and electromagnetic skin-depth effects at about 1 mm, to larger-scale fluid-like phenomena (extending over a few centimeters). The fluid-like models resemble resistive MHD models but also include semikinetic plasma-flow vorticity and micromagnetic island-generation mechanisms. In the smaller-scale-length models the various effects on vorticity generation often must be calculated kinetically; they include wave–particle energy transfer effects (Landau damping), trapped-particle effects, finite gyro-radius effects and others. For scale lengths on the order of the ion gyro radius or smaller, the $\mathbf{E}\times\mathbf{B}/B^2$ flow response of the ions is reduced. A gyrokinetic formalism is required in those cases, and the usual plasma flow vorticity is no longer a meaningful quantity.

Considerable effort over the past two decades has been put into developing a linear theory of these various types of microinstabilities. However, very few studies of core plasma turbulence and transport have gone beyond dimensional analysis based on turbulent mixing-length arguments. The transport levels so estimated can be comparable to the observed transport, but at present no model or combination of models seems to explain anomalous transport in the hot core of tokamak plasmas.

The limited experimental data on core fluctuations, particularly those that have recently become available, indicate nearly ubiquitous and featureless spectra peaked

at low perpendicular wavenumbers and frequencies. While all the phenomena discussed in the preceding two paragraphs are operative in some region of the spectrum, in the plasma rest frame the largest fluctuations seem to have perpendicular correlation lengths of a few centimeters and low frequencies that are approximately the same order as the collision frequencies.

Numerical calculations

For both core and edge plasmas, numerical studies have played an important role in broadening our knowledge of plasma turbulence. Plasma turbulence involves a broad range of space and time scales; thus numerical resolution strongly constrains the range of parameters that can be studied. For tokamak plasmas, the strong toroidal magnetic field is a source of anisotropy for the turbulence. The parallel, mostly toroidal, coherence length of fluctuations is always much greater than the radial and poloidal lengths. The turbulence spectrum tends to be localized in a narrow band in m/n space near the local winding number. Thus plasma turbulence in tokamaks is quasi-two-dimensional and localized in its radial extent, although dynamically it is fully three dimensional. Hence these numerical calculations are somewhat easier than for classical fluid turbulence. Nonetheless, they are clearly at the "grand challenge" level of computation.

Joint analytical and numerical studies of plasma turbulence have led in recent years to an understanding of some key issues in the physics of turbulence in magnetized plasmas—for example, the poloidal flow shear effects shown in figure 7. It has been possible to use and further develop some of the renormalization techniques developed for neutral fluids. Also, some of the basic dynamical mechanisms for saturation of the turbulence have been unraveled. For instance, for resistive MHD thermal instabilities induced by a gradient in the resistivity, linear instability occurs when the thermal perturbation grows rapidly compared with its rate of equilibration along the magnetic field. The instability saturates nonlinearly because the parallel heat diffusion is enhanced by turbulent radial diffusion and balances the instability drive. Thus "resonance broadening" in space produces the saturation.[19] It has also been shown that while the mixing-length model, which is the simplest model of turbulence and transport, can give the scaling of the fluctuation amplitude and the induced transport at saturation, a direct-interaction-approximation type of renormalization theory is needed to predict their absolute levels.[20]

While the macroscopic stabilization of tokamak plasmas is sufficiently well characterized and understood that it can be used to explore higher-performance and burning-plasma operating regimes, developing an understanding of tokamak plasma turbulence and transport remains a major scientific challenge. It is certainly one of the outstanding physics conundrums of the late 20th century. Solving it, together with exploring higher-β, steady-state and burning-plasma operating regimes, is quite important for optimizing tokamak reactors and enhancing the prospects for fusion energy.

References

1. F. F. Chen, *Introduction to Plasma Physics and Controlled Fusion*, 2nd ed., Plenum, New York (1984). J. A. Bittencourt, *Fundamentals of Plasma Physics*, Pergamon, Oxford (1986).
2. See I. E. Tamm, A. D. Sakharov, in *Plasma Physics and the Problem of Controlled Thermonuclear Reactions*, vol. 1, M. A. Leontovich, ed., Pergamon, New York (1961), p. 1.
3. L. Spitzer Jr, in report WASH-115, US Atomic Energy Commission (1952), p. 12.
4. L. A. Artsimovich, Nucl. Fusion **12**, 215 (1972). J. Wesson, *Tokamaks*, Clarendon, Oxford (1987). R. B. White, *Theory of Tokamak Plasmas*, North–Holland, Amsterdam (1989).
5. H. Grad, H. Rubin, in *Theoretical and Experimental Aspects of Controlled Nuclear Fusion*, Proc. Second UN Int. Conf. on the Peaceful Uses of Atomic Energy, vol. 31, United Nations, Geneva (1958), p. 190. V. D. Shafranov, Sov. Phys. JETP **26**, 682 (1960); Sov. J. At. En. **13**, 1149 (1963).
6. J. P. Freidberg, *Ideal Magnetohydrodynamics*, Plenum, New York (1987), p. 258ff. G. Schmidt, *Physics of High Temperature Plasmas*, 2nd ed., Academic, New York (1979), chs. 4 and 5.
7. L. C. Bernard, F. J. Helton, R. W. Moore, T. N. Todd, Nucl. Fusion **23**, 1475 (1983). F. T. Troyon, R. Gruber, H. Sauremann, S. Semengato, S. Succi, Plasma Phys. Controlled Fusion **26**, 209 (1984). A. Sykes, M. F. Turner, S. Patel, in *Proc. Eleventh European Conf. Controlled Fusion and Plasma Phys.*, vol. 2, European Phys. Soc., Petit-Lancy, Switzerland (1983), p. 363.
8. For high-β experiments on the ISX-B tokamak, see G. H. Neilson *et al.*, Nucl. Fusion **23**, 285 (1983). For the DIII tokamak experiments, see K. H. Burrell *et al.*, Nucl. Fusion **23**, 536 (1983). For a discussion of the scaling described by equation 1, see R. D. Stambaugh *et al.*, in *Plasma Physics and Controlled Nuclear Fusion Research 1984*, vol. 1, Int. Atomic Energy Agency, Vienna (1985), p. 217. For PBX-M tokamak experiments, see N. Sauthoff *et al.*, in *Plasma Physics and Controlled Nuclear Fusion Research 1990*, vol. 1, Int. Atomic Energy Atomic, Vienna (1991), p. 709. For the DIII-D tokamak experiments, see E. A. Lazarus *et al.*, Phys. Fluids B **3**, 2220 (1991).
9. B. Coppi, A. Ferreira, J. W.-K. Mark, J. J. Ramos, Nucl. Fusion **19**, 715 (1979). C. Mercier, in *Plasma Physics and Controlled Nuclear Fusion Research 1978*, vol. 1, Int. Atomic Energy Agency, Vienna (1979), p. 701. P. J. Fielding, F. A. Haas, *ibid.*, p. 630. D. Lortz, J. Nuhrenburg, Phys. Lett. A **68**, 49 (1978).
10. H. P. Furth, J. Killeen, M. N. Rosenbluth, Phys. Fluids **6**, 459 (1963). J. D. Callen *et al.*, in *Plasma Physics and Controlled Nuclear Fusion Research 1978*, vol. 1, Int. Atomic Energy Agency, Vienna (1979), p. 415. H. P. Furth, Phys. Fluids **28**, 1595 (1985).
11. J. D. Callen, "Transport Processes in Magnetically Confined Plasmas," U. Wisc. report CPTC 91-18 (December 1991), to be published in Phys. Fluids B. J. D. Callen *et al.*, Phys. Fluids B **2**, 2869–2960 (1990).
12. F. L. Hinton, R. D. Hazeltine, Rev. Mod. Phys. **48**, 239 (1976). S. P. Hirshman, D. J. Sigmar, Nucl. Fusion **21**, 1079 (1981).
13. For work on MACROTOR, see S. J. Zweben, R. J. Taylor, Nucl. Fusion **21**, 193 (1981). For recent, comprehensive studies on TEXT, see C. P. Ritz *et al.*, Phys. Rev. Lett. **62**, 1844 (1989).
14. C. P. Ritz *et al.*, in *Plasma Physics and Controlled Nuclear Fusion Research 1990*, vol. 2, Int. Atomic Energy Agency, Vienna (1991), p. 589.
15. H. Biglari, P. H. Diamond, P. W. Terry, Phys. Fluids B **2**, 1 (1990).
16. K. C. Shaing, E. C. Crume Jr, Phys. Rev. Lett. **63**, 2369 (1989).
17. R. J. Groebner, K. H. Burrell, R. P. Seraydarian, Phys. Rev. Lett. **64**, 3015 (1990).
18. R. J. Taylor *et al.*, Phys. Rev. Lett. **63**, 2365 (1989).
19. L. Garcia, P. H. Diamond, B. A. Carreras, J. D. Callen, Phys. Fluids **28**, 2147 (1985).
20. P. H. Diamond, B. A. Carreras, Comments Plasma Phys. Controlled Fusion **10**, 271 (1987). B. A. Carreras, L. Garcia, P. H. Diamond, Phys. Fluids **30**, 1388 (1987).
21. Y. Nagayama *et al.*, "ECE and X-Ray Image Reconstructions of Sawtooth Oscillations on TFTR," report PPPL-2773, Princeton Plasma Phys. Lab., Princeton, N. J. (October 1991), to be published in Phys. Rev. Lett.
22. L. C. Bernard, F. J. Helton, R. W. Moore, Comput. Phys. Commun. **24**, 377 (1981).
23. J. N. Leboeuf *et al.*, Phys. Fluids B **3**, 2291 (1991). ■